Preparation and structural characterisation of magnetic $NiFe_2O_4$@ABS@Ag nanocompound with antibacterial property

Maryam Mohebbi[1], *Alireza Allafchian*[2] ✉, *Parviz Kameli*[1], *Seyed Amirhoosien Jalali*[3,4]

[1]*Department of Physics, Isfahan University of Technology, Isfahan 84156–83111, Iran*
[2]*Research Institute for Nanotechnology and Advanced Materials, Isfahan University of Technology, Isfahan 84156–83111, Iran*
[3]*Research Institute for Biotechnology and Bioengineering, Isfahan University of Technology, Isfahan 84156–83111, Iran*
[4]*Department of Natural Resources, Isfahan University of Technology, Isfahan 84156–83111, Iran*
✉ *E-mail: allafchian@cc.iut.ac.ir*

Published in Micro & Nano Letters; Received on 16th May 2018; Revised on 16th September 2018; Accepted on 20th December 2018

The present research attempted to characterise the structural and magnetic characteristics of $NiFe_2O_4$@ABS@Ag nanoparticles (NPs) made of nickel ferrite ($NiFe_2O_4$), acrylonitrile butadiene styrene (ABS) and silver NPs (Ag NPs), this was done by employing techniques such as X-ray diffraction (XRD), Fourier transform infrared spectroscopy, scanning electron microscopy and transmission electron microscopy, as well as a vibrating sample magnetometer. The XRD patterns obtained indicated that following ABS and Ag NPs coating, the crystallite size (from Scherrer formula) was increased from 32 to 40 nm. It was confirmed by the magnetic measurements that the maximum magnetisation of the $NiFe_2O_4$ core was dropped when the surface was coated with ABS and Ag NPs. The antimicrobial activity of this three-component nanocomposite was tested, showing that the nanocomposite $NiFe_2O_4$@ABS@Ag could be isolated from a water solution by using a magnet.

1. Introduction: In recent years, confronting the water contamination problems, including bacteria, has been attracted much attention. Metallic nanoparticles (NPs) have been proved to be excellent antimicrobial agents. Among the numerous NPs used as microbial agents, the Ag NPs are the famous antibacterial agent due to their higher antimicrobial activities against bacteria. The most important issue in microbial contamination is bringing the antibacterial agent to the bacteria containing medium while preventing its effects on the environment. Magnetic NPs of iron oxides are known as one member of the most accessible nomination used for the provision of magnetic NPs, this is due to their suitable magnetic properties as well as their low price [1]. However, because of their large ratio of surface area/volume, the magnetic NPs of iron oxide cores are likely to gather, thereby losing the individual properties which are associated with their initial nanometre dimensions. Consequently, suitable surface repair and particle stabilisation are important challenges encountered when the goal is to extend the utility of magnetic NPs to bioapplications [2].

It has been revealed by recent studies that polymers can be effective in the synthesis and long permanent adjunction of metal NPs. It has been revealed that the polymer network around the magnetic core can fixate NPs through the electrostatic interaction of their functional groups [3]. Accordingly, numerous polymers have been developed as antibacterial Ag NPs supports. In this regard, polymers such as polyaniline and polyacrylonitrile co-maleic anhydride and polymethyl methacrylate have been the focus of some studies [4–7]. The acrylonitrile butadiene styrene (ABS) is known as a strong and durable production grade thermoplastic employed in many different industries. The ABS polymers are noteworthy as they are widely used in many house hold items; they are also cheaper than other polymers. The ABS plastics have been observed to exhibit good durability and resilience; they have also been reported to have good mechanical strength. In addition, it has been revealed that these thermoplastic polymers ensure the favourable combination of thermal, electrical and mechanical properties [8].

Recently, combining magnetic NPs with a silver nanoshell has been of much interest owing to its stability, durability, strong antimicrobial activity, thereby warding many different bacteria and the relatively low toxicity to humans [9].

In the present research, in order to omit Ag NPs of environment that is limited in the use of them and increase the antibacterial Ag NPs, a novel kind of three-component magnetic nanocompound with a core/shell/shell structure called $NiFe_2O_4$@ABS@Ag was developed. $NiFe_2O_4$ was synthesised by employing the citrate-gel method [10, 11]; then it was coated with the ABS polymer to obtain the $NiFe_2O_4$@ABS compound. As the final step, Ag NPs provided by the reduction of Ag^+ ions were convened in the surface of the $NiFe_2O_4$@ABS composite in order to obtain the final $NiFe_2O_4$@ABS@Ag nanocompound. The characterisation of this nanocompound was done by employing a varied method, then its antibacterial activity was subjected to testing for different bacteria. $NiFe_2O_4$@ABS@Ag nanocompound was found to have stronger antibacterial properties in comparison with bare Ag NPs.

2. Laboratory processes

2.1. Required materials: The chemicals used in the study are Ni $(NO_3)_2$, $Fe(NO_3)_3$, $Ag(NO_3)$, $K_2S_2O_8$, Na_2SO_3, NaOH and ABS; all the chemicals were of analytical grade provided by Merck and used as-received without further purification.

2.2. Synthesis

2.2.1. Synthesis of $NiFe_2O_4$: For the preparation of $NiFe_2O_4$ NPs, at first, 5 g of $Fe(NO_3)_3{\cdot}9H_2O$ was solvate in 20 ml of deionised water; then 1.7 g $Ni(NO_3)_2{\cdot}6H_2O$ and 1.2% citric acid were dissolved in 20 ml of deionised water and the two solutions were mixed. Then, ammonium hydroxide was allowed to be added to the reaction, with the pH value reaching 9. After that, the mixture was stirred at 30°C for 2 h and then dried in an oven at 100°C for 24 h. Finally, it was calcined in an argon atmosphere at 600°C for 2 h.

2.2.2. Synthesis of $NiFe_2O_4$@Ag: To prepare $NiFe_2O_4$@Ag NPs, as the first step, 1.0 g of $NiFe_2O_4$ was dispersed in 0.189 g of $AgNO_3$ solution; then the mixture was allowed to be stirred for 2 h and sonicated for 15 min. Following that, while stirring the solution slowly, 50 ml of 10.0 mmol l^{-1} of sodium borohydrate, was added drop-wise into the solution. The provided $NiFe_2O_4$@Ag NPs were washed with distilled water twice, then they were placed in an oven at 60°C for 6 h.

2.2.3. Synthesis of $NiFe_2O_4$@ABS nanocomposite: For the preparation of the $NiFe_2O_4$@ABS composite, ABS was precipitated on the surface of pre-synthesised $NiFe_2O_4$ NPs. Initially, 0.205 g ABS polymer was dissolved in a minimum amount of Dimethylformamide (DMF) (1.0 g ABS was added into 2.0 ml of DMF at 40°C). The solution was allowed to be stirred for 6 h in order to dissolve the ABS polymers completely); then, the reaction mixture was added to 1.0 g of nickel ferrite at room temperature, solicited for 1 h; subsequently, it was dried in the oven at 60°C for 6 h.

2.2.4. Synthesis of $NiFe_2O_4$@ABS@Ag nanocomposite: The synthesis of $NiFe_2O_4$@ABS composite was done in 20 ml $AgNO_3$ aqueous solution. After stirring for 2 h, it was sonicated for 15 min and the whole mixture was stirred; following that, a solution of sodium borohydride was added drop-wise into the solution. Later, the provided $NiFe_2O_4$@ABS@Ag nanocompound was separated and allowed to be washed various times with water in order to eliminate any over plus protecting agent. Finally, this nanocompound was obtained by drying in an oven at 60°C for 6 h.

2.3. Characterisation: The elemental ratio of each of the provided non-magnetic composites was investigated using a Hitachi Japan S4160 scanning electron microscopy with an energy dispersive X-ray spectroscopy. X-ray diffraction (XRD) pattern was carried out on the Philips X–ray diffract meter (Cu K radiation ($\lambda = 0.154$ nm)), in the steps of size 0.02. A continuous scan mode was then employed to collect 2θ range from 10° to 80°.

In order to study and address the magnetic properties of the as-provided compounds, the vibrating sample magnetometer (VSM) from Magnates Dogfight Kavir Company was utilised. The surface area of all samples was characterised by using the single-point Brunauer–Emmett–Teller (BET; Nano Sord, Iran) technique. An ultrasonic homogeniser device (20 Hz 150 W, Iran) with a 25 mm probe from Tosee Mafoge Soot Company was used for opening the agglomerated nanocomposite.

2.4. Antibacterial tests: Disk diffusion tests were employed to investigate the bacterial sensitivities of *Escherichia coli* (ATCC 35218), *Salmonella typhimurium* (ATCC 14028), *Staphylococcus aureus* (ATCC 29213) and *Bacillus cereus* (ATCC 14579) to all the provided magnetic composites. The solution (0.05 g of substance in 0.5 ml sterile water) was ultrasonicated for 20 min; then by adding 30 ml of each of the prepared magnetic NPs suspension to disks with 6 mm in diameter, they were placed on a Mueller–Hinton agar culture medium (Merck, Germany) which was smeared by the standard bacterial species. Diameters of the disks were measured using a ruler with the accuracy of 1 mm. Based on six replicates, the mean inhibition zones' diameters and standard deviations of each microbial strain were determined [12, 13].

3. Results and discussion

3.1. Analysis of Fourier transform infrared (FTIR) result: The IR spectra were recorded in the range of 2700–400 cm^{-1} and at the ambient temperature as shown in Fig. 1. In all of the spectrum, two major absorbency peaks at 579 and 453 cm^{-1} that corresponded to the intrinsic stretching vibrations of Fe ions in tetrahedral and octahedral sites of the spinel structure, respectively, could be displayed. However, as shown in Fig. 1, the FTIR spectrum of $NiFe_2O_4$@ABS and $NiFe_2O_4$@ABS@Ag nanocompounds exhibited all specifications peaks of ABS, as well as the Fe–O stretching vibrations [14, 15]. The peak at 996 cm^{-1} corresponded to the O–H stretching vibration and the C = O, respectively. Also, it must be noted that the peak at 2238 cm^{-1} referred to C≡N stretching vibrations [16]. However, the height peak at 1640 cm^{-1} was related to the carbonyl groups of carboxylic acid in $NiFe_2O_4$@ABS. This indicated that this peak was reduced in the spectra of $NiFe_2O_4$@ABS@Ag; this was because of the interplay

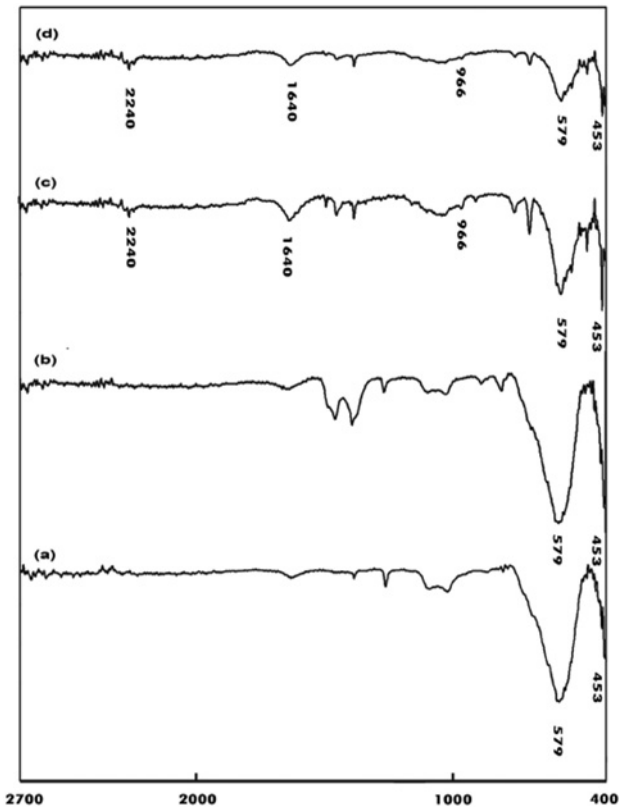

Fig. 1 *FTIR spectra of*
a $NiFe_2O_4$
b $NiFe_2O_4$@Ag
c $NiFe_2O_4$@ABS
d $NiFe_2O_4$@ABS@Ag

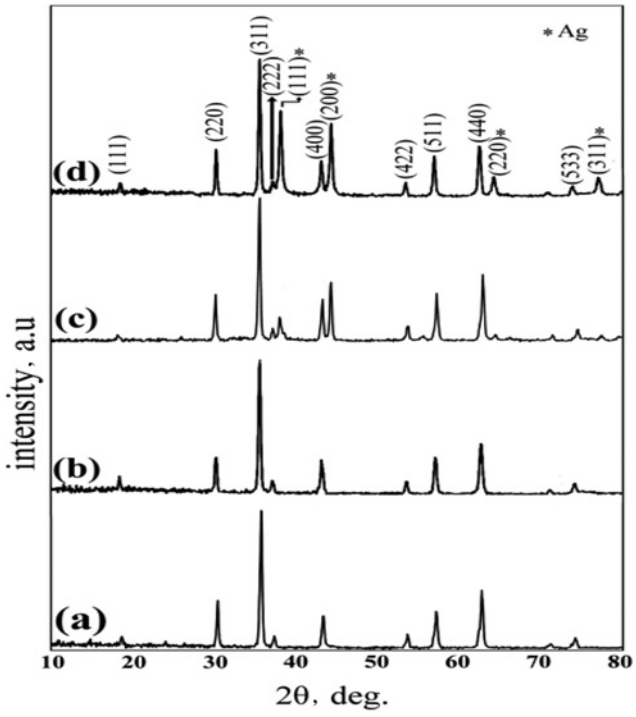

Fig. 2 *XRD patterns of*
a $NiFe_2O_4$
b $NiFe_2O_4$@ABS
c $NiFe_2O_4$@Ag and
d $NiFe_2O_4$@ABS@Ag

doi: 10.1049/mnl.2018.5175

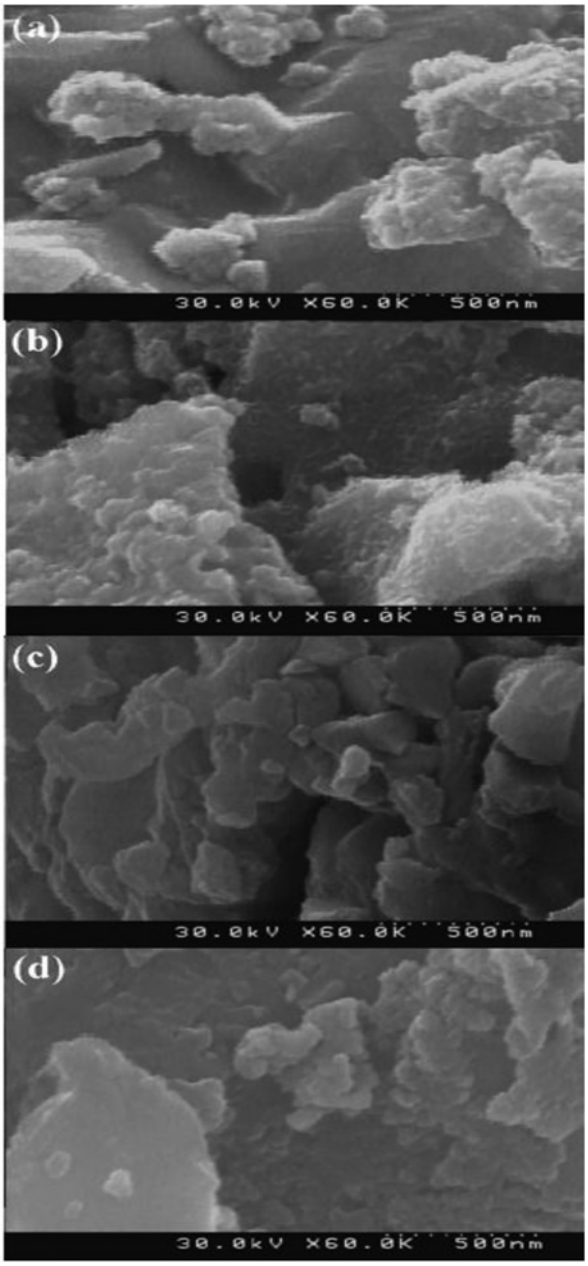

Fig. 3 *FESEM images of*
a $NiFe_2O_4$
b $NiFe_2O_4$@Ag
c $NiFe_2O_4$@ABS and
d $NiFe_2O_4$@ABS@Ag

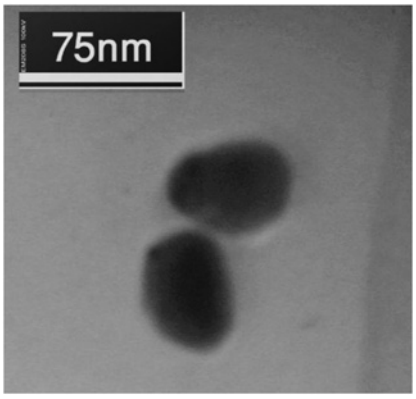

Fig. 4 *TEM image of the three-component $NiFe_2O_4$@ABS@Ag composite*

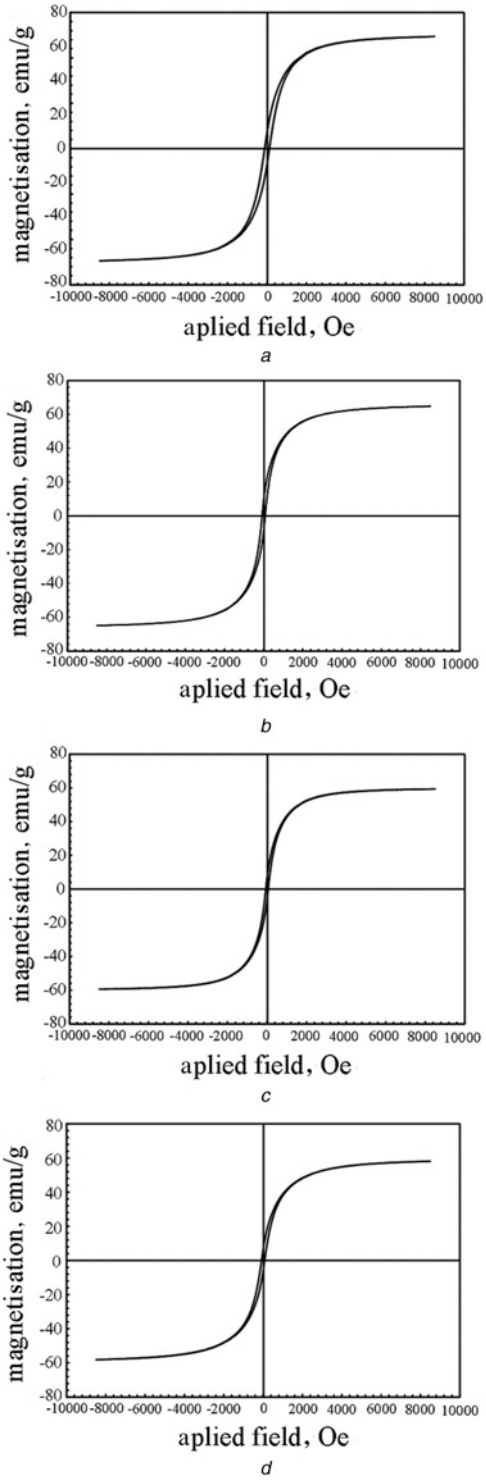

Fig. 5 *VSM curves of*
a $NiFe_2O_4$
b $NiFe_2O_4$@ABS
c $NiFe_2O_4$@Ag
d $NiFe_2O_4$@ABS@Ag

Table 1 Magnetic parameters of $NiFe_2O_4$, $NiFe_2O_4$@Ag, $NiFe_2O_4$@ABS and $NiFe_2O_4$@ABS@Ag nanocomposites measured by using a VSM

Compounds	H_c, O_e	M_r, emu/g	M_S, emu/g
$NiFe_2O_4$	79	9	65
$NiFe_2O_4$@Ag	78	6	58
$NiFe_2O_4$@ABS	75	6	56
$NiFe_2O_4$@ABS@Ag	74	7	56

Table 2 Zone of inhibition (mm) of $NiFe_2O_4$, $NiFe_2O_4$@ABS, $NiFe_2O_4$@Ag, and $NiFe_2O_4$@ABS@Ag against tested bacteria

Compounds	Zone of inhibition (mm) average ± standard deviation			
	S. aureus	*B. cereus*	*E. coli*	*S. typhimurium*
distilled water	6.4	6.4	6.4	6.4
$NiFe_2O_4$	6.4	6.4	6.4	6.4
$NiFe_2O_4$@Ag	13	10	11	12
$NiFe_2O_4$@ABS	6.4	6.4	6.4	6.4
$NiFe_2O_4$@ABS@Ag	19	21	16	19

among the carbonyl groups of the carboxylic acid of the polymer and Ag atoms.

3.2. Analysis of XRD results: The crystal structure of NPs was confirmed, as revealed by XRD patterns that were recorded for $NiFe_2O_4$, $NiFe_2O_4$@Ag, $NiFe_2O_4$@ABS, and $NiFe_2O_4$@ABS@Ag NPs. In the pattern of $NiFe_2O_4$, as can be seen in Fig. 2. Nine diffraction peaks were observed at a 2θ value of 18.42°, 30.3°, 35.65°, 37.29°, 43.26°, 53.61°, 57.16°, 62.74° and 74.24°, corresponding to diffraction from the (111), (220), (311), (222) (400), (422), (511), (440), and (533), respectively. The scriptable peaks showed the main diffraction patterns that could be characterised for spinel $NiFe_2O_4$ in JCPDS Card No. 44–1485. The crystallite size $NiFe_2O_4$ particles were estimated to be around 32 nm, by using Debye–Scherrer formula, according to the XRD data [17, 18]. The XRD patterns of the $NiFe_2O_4$@ABS nanocompound illustrated diffraction peaks which were similar to those of the free $NiFe_2O_4$ core. This indicated that the spinel structure of $NiFe_2O_4$ stayed unchanged after covering of ABS. Four peaks for Ag^+ were also seen at 2θ of 37.34°, 44.52°, 63.08° and 76.32° for the $NiFe_2O_4$@ABS@Ag nanocomposite, corresponding to (*hkl*) planes of (111), (200), (220), and (311), which were in agreement with the data in the JCPDS file (JCPDS Card No. 4–783) [19, 20].

3.3. Analysis of field emission scanning electron microscopy (FESEM) result: The surface morphologies of all compounds can be observed in Fig. 3. FESEM images of $NiFe_2O_4$ and $NiFe_2O_4$@Ag NPs showed that NPs appeared as a porous foam-like structure, owing to citrate–gel synthesis [21]; on the other hand, the FESEM micrographs of $NiFe_2O_4$@ABS and $NiFe_2O_4$@ABS@Ag compounds demonstrated different images with sphere-like structures having fewer aggregating that attributed to the interaction of $NiFe_2O_4$ NPs due to the coating of ABS [18, 22].

3.4. Analysis of transmission electron microscopy (TEM) result: For further exploration of the morphology of the $NiFe_2O_4$@ABS@Ag nanocompound, TEM was conducted. The TEM image demonstrated that Ag NPs are visible as black spherical points on the grey shell of the ABS coverage, this image clearly indicated the core–shell state as shown in Fig. 4.

3.5. Analysis of BET result: It is commonly reported that surface areas of all nanocompounds were measured by using the BET theory. It was revealed from the BET data that the surface area of $NiFe_2O_4$ NPs, $NiFe_2O_4$@Ag, $NiFe_2O_4$@ABS, and $NiFe_2O_4$@ABS@Ag nanocompounds was 74.2, 41.4, 42.2 and 37.4 m^2/g, respectively. The results have shown that by covering the magnetic core with ABS and ABS@Ag and filling hole and enlarging, the surface area of $NiFe_2O_4$@ABS@Ag was reduced due to the embedding of ABS and ABS@Ag into the core [23].

3.6. Analysis of VSM result: In order to characterise the magnetic properties of all nanocompounds, the VSM was employed at room temperature. The magnetisation curves of $NiFe_2O_4$Nps, $NiFe_2O_4$@Ag, $NiFe_2O_4$@ABS, and $NiFe_2O_4$@ABS@Ag NPs can be seen in Fig. 5. The maximum magnetisation value (M_s), coercivity (H_c) and remanence magnetisation (M_r) of samples could be defined based on the hysteresis loops measurements and can be seen in Table 1. The M_s, M_r and H_c values obtained after Ag and ABS coating were less than the $NiFe_2O_4$ core, decreasing in M_s and M_r values was owing to non-magnetic ABS and Ag NPs coverage on the $NiFe_2O_4$ magnetic core, this led to decreasing the magnetic strength of the NPs, while Ag and ABS increased the crystallite size of the $NiFe_2O_4$@ABS@Ag nanocomposite, results showed that the coercivity (H_c) value has also been decreased, it may be due to the surface anisotropy [24–26]. It was found, however, that the value M_s of the $NiFe_2O_4$ core was significantly reduced, the $NiFe_2O_4$@ABS@Ag compound could still be easily separated from media with the application of an external magnetic field.

3.7. Antibacterial test: Despite the strong antibacterial property of silver, cytotoxic activity against mammalian cells could lead to some limitations in the use of them as the remedial agent [27, 28]. Therefore, the omission Ag NPs of environment that is limited their usages. By employing the nanocompound $NiFe_2O_4$@Ag and $NiFe_2O_4$@ABS@Ag as the antiseptic agent, in lieu of Ag NPs, this compound could be separated from the media by the magnet. Therefore, investigation of the bactericidal properties of $NiFe_2O_4$@Ag and $NiFe_2O_4$@ABS@Ag nanocompounds could be useful. As shown in Table 2 and Fig. 6, the

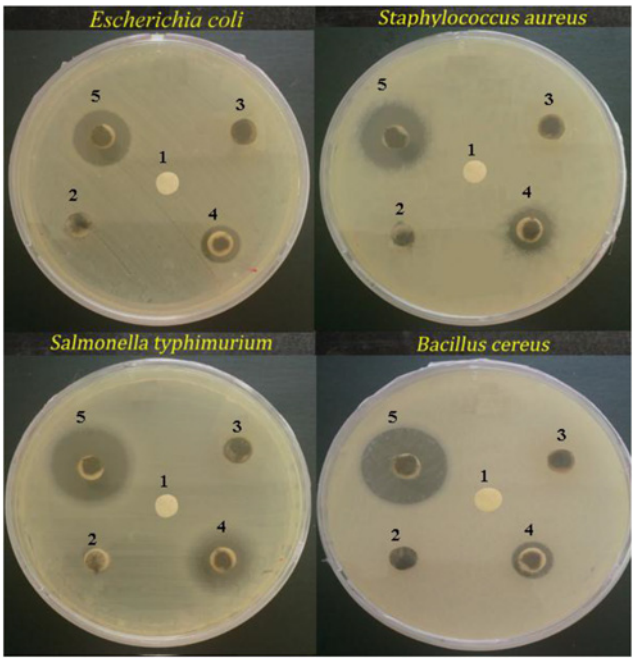

Fig. 6 *Zone of inhibition of 1: blank disks; 2: $NiFe_2O_4$; 3: $NiFe_2O_4$@ABS; 4: $NiFe_2O_4$@Ag; 5: $NiFe_2O_4$@ABS@Ag against tested bacteria*

doi: 10.1049/mnl.2018.5175

antimicrobial activity of the $NiFe_2O_4$@ABS@Ag nanocompound was higher than that of $NiFe_2O_4$ and $NiFe_2O_4$@ABS, as well as that of $NiFe_2O_4$@Ag nanomaterials.

4. Conclusion: The $NiFe_2O_4$ NPs were fixed as a magnetic core and decorated the ABS layer on the surface of this core in the inner shell, then decorated Ag NPs on the surface of $NiFe_2O_4$@ABS in the outer shell to yield a novel kind of three components $NiFe_2O_4$@ABS@Ag NPs with a core/shell/shell structure. This nanocompound was studied using XRD, TEM, BET, FTIR, and FESEM techniques. It was found that supporting Ag NPs on ABS-coated $NiFe_2O_4$ led to preventing aggregation. The magnetic properties were investigated by employing VSM, indicating that the M_s and M_r values of $NiFe_2O_4$ core were decreased upon coating with ABS and Ag NPs. The antimicrobial investigation of $NiFe_2O_4$@ABS@Ag nanocompound indicated that it was higher than $NiFe_2O_4$, $NiFe_2O_4$@ABS and $NiFe_2O_4$@Ag. Their comparison with antibacterial properties of nanocomposites made in this project and similar nanocomposite made by others showed an increase in the antibacterial properties of this material relative to the nanocomposites made before, which shows the innovation and acceptability of nanocomposites in this study [4, 24, 29]. Interestingly, this nanocompound could be, therefore, conveniently separated from the solution by applying a magnetic field.

5 References

[1] Peng S., Wang C., Xie J., *ET AL.*: 'Synthesis and stabilization of monodisperse Fe nanoparticles', *J. Am. Chem. Soc.*, 2006, **128**, pp. 10676–10677

[2] Sun C., Lee J., Zhang M.: 'Magnetic nanoparticles in MR imaging and drug delivery', *Adv. Drug Deliv.*, 2008, **60**, pp. 1252–1265

[3] Zhang R., Lin W., Moon K.S., *ET AL.*: 'Fast preparation of printable highly conductive polymer nanocomposites by thermal decomposition of silver carboxylate and sintering of silver nanoparticles', *ACS Appl. Mater. Interfaces*, 2010, **2**, pp. 2637–2645

[4] Kooti M., Kharazi P., Motamedi H.: 'Preparation and antibacterial activity of three-component $NiFe_2O_4$@PANI@Ag nanocomposite', *J. Mater. Sci. Technol.*, 2014, **30**, pp. 656–660

[5] Allafchian A.R., Jalali S.A.H., Bahramian H., *ET AL.*: 'Preparation, characterization, and antibacterial activity of $NiFe_2O_4$/PAMA/Ag–TiO_2 nanocomposite', *J. Magn. Magn. Mater.*, 2016, **404**, pp. 14–20

[6] Allafchian A.R., Bahramian H., Jalali S.A.H., *ET AL.*: 'Synthesis, characterization and antibacterial effect of new magnetically core–shell nanocomposites', *J. Magn. Magn. Mater.*, 2015, **394**, pp. 318–324

[7] Kong H., Jang J.: 'Antibacterial properties of novel poly (methyl methacrylate) nanofiber containing silver nanoparticles', *Langmuir*, 2008, **24**, pp. 2051–2056

[8] Rutkowski V., Levintus C.: 'Acroylonitrile-Butadiene-Styrene Copolymers (ABS): Pyrolysis and Combustion Products and their Toxicity-A Review of the Literature', *Fire and Mater.*, 1986, **10**, pp. 93–105

[9] Asharani P., Gong Z., Wu Y.L., *ET AL.*: 'Toxicity of silver nanoparticles in Zebrafish models', *Nanotechnology*, 2008, **19**, p. 255102

[10] Mirahmadi-Zare S.Z., Allafchian A., Aboutalebi F., *ET AL.*: 'Super magnetic nanoparticles $NiFe_2O_4$, coated with aluminum–nickel oxide sol–gel lattices to safe, sensitive and selective purification of his-tagged proteins', *Protein Expression Purif.*, 2016, **121**, pp. 52–60

[11] Mirahmadi-Zare S.Z., Aboutalebi F., Allafchian M., *ET AL.*: 'Layer by layer coating of NH_2-silicate/polycarboxylic acid polymer saturated by Ni^{2+} onto the super magnetic $NiFe_2O_4$ nanoparticles for sensitive and bio-valuable separation of His-tagged proteins', *Protein Expression Purif.*, 2018, **143**, pp. 71–76

[12] Melaiye A., Sun Z., Hindi K., *ET AL.*: 'Silver (I)-imidazole cyclophane gem-diol complexes encapsulated by electrospun tecophilic nanofibers: formation of nanosilver particles and antimicrobial activity', *J. Am. Chem. Soc.*, 2005, **127**, pp. 2285–2291

[13] Allafchian A.R., Jalali S.A.H., Amiri R., *ET AL.*: 'Synthesis and characterization of the $NiFe_2O_4$@TEOS–TPS@Ag nanocomposite and investigation of its antibacterial activity', *Appl. Surf. Sci.*, 2016, **385**, pp. 506–514

[14] Ensafi A.A, Arashpour B., Rezaei B., *ET AL.*: 'Voltammetric behavior of dopamine at a glassy carbon electrode modified with $NiFe_2O_4$ magnetic nanoparticles decorated with multiwall carbon nanotubes', *Mater. Sci. Eng. C*, 2014, **39**, pp. 78–85

[15] Salari D., Ranjbar H.: 'Study on the recycling of ABS resins: simulation of reprocessing and thermo-oxidation', *Iran. Polym. J.*, 2008, **17**, pp. 559–610

[16] Kim S.S., Lee J.: 'Antibacterial activity of polyacrylonitrile–chitosan electrospun nanofibers', *Carbohydr. Polym.*, 2014, **102**, pp. 231–237

[17] Ensafi A.A., Saeid B., Rezaei B., *ET AL.*: 'Differential pulse voltammetric determination of methyldopa using MWCNTs modified glassy carbon decorated with $NiFe_2O_4$ nanoparticles', *Ionics*, 2015, **21**, (5), pp. 1435–1444

[18] Senthilkumar B., Sankar K.V., Sanjeeviraja C., *ET AL.*: 'Synthesis and physico-chemical property evaluation of PANI–$NiFe_2O_4$ nanocomposite as electrodes for supercapacitors', *J. Alloys Compd.*, 2013, **553**, pp. 350–357

[19] Allafchian A., Farhang H., Jalali S.A.H., *ET AL.*: '*Gundelia tournefortii* L.: a natural source for the green synthesis of silver nanoparticles', *IET Nanobiotechnol.*, 2017, **11**, (7), pp. 815–820

[20] Khatami M., Alijani H.Q., Nejad M.S., *ET AL.*: 'Core@shell nanoparticles: greener synthesis using natural plant products', *Appl. Sci.*, 2018, **8**, (3), p. 411

[21] Priyadharsini P., Pradeep A., Rao P.S., *ET AL.*: 'Structural, spectroscopic and magnetic study of nanocrystalline Ni–Zn ferrites', *Mater. Chem. Phys.*, 2009, **116**, pp. 207–213

[22] Li L., Jiang J., Xu F.: 'Preparation, characterization and magnetic properties of PANI/La-substituted LiNi ferrite nanocomposites', *Chin. J. Chem.*, 2006, **24**, pp. 1804–1809

[23] Lee K.H., Lee B., Lee K.R., *ET AL.*: 'Dual Pd and $CuFe_2O_4$ nanoparticles encapsulated in a core/shell silica microsphere for selective hydrogenation of arylacetylenes', *Chem. Commun.*, 2012, **48**, pp. 4414–4416

[24] Kooti M., Kharazi P., Motamedi H.: 'Preparation, characterization, and antibacterial activity of $CoFe_2O_4$/polyaniline/Ag nanocomposite', *J. Taiwan Inst. Chem. Eng.*, 2014, **45**, pp. 2698–2704

[25] Guo P., Cui L., Wang Y., *ET AL.*: 'Facile synthesis of $ZnFe_2O_4$ nanoparticles with tunable magnetic and sensing properties', *Langmuir*, 2013, **29**, pp. 8997–9003

[26] Batlle X., Labarta A.: 'Finite-size effects in fine particles: magnetic and transport properties', *J. Phys. D, Appl. Phys.*, 2002, **35**, pp. R15–R42

[27] Chudasama B., Vala A.K., Andhariya N., *ET AL.*: 'Enhanced antibacterial activity of bifunctional Fe_3O_4–Ag core–shell nanostructures', *Nano Res.*, 2009, **2**, pp. 955–965

[28] Beer C., Foldbjerg R., Hayashi Y., *ET AL.*: 'Toxicity of silver nanoparticles-nanoparticle or silver ion', *Toxicol. Lett.*, 2012, **208**, pp. 286–292

[29] Kooti M., Saiahi S., Motamedi H.: 'Fabrication of silver-coated cobalt ferrite nanocomposite and the study of its antibacterial activity', *J. Magn. Magn. Mater.*, 2013, **333**, pp. 138–143